Advanced halide/sulfide all-solid-state lithium metal batteries with fluorinated interface layer

Shuangwu Xu,[a] Na Chen,[a] You Huang,[a] Dan Sun,[a] Huanhuan Li,[b] Huapeng Sun,[c] Zhiguang Peng,[a]* Yougen Tang,[a] Hehe Zhang,[d]* and Haiyan Wang [a]*

[a] Hunan Provincial Key Laboratory of Chemical Power Sources, College of Chemistry and Chemical Engineering, Central South University, Changsha 410083, China

[b] School of Chemistry and Chemical Engineering, Henan Normal University, Xinxiang 453007, P. R. China

[c] School of New Energy, Chenzhou Vocational Technical College; Chenjiang Laboratory, Chenzhou, Hunan 423000, China

[d] School of Energy and Mechanical Engineering, Nanjing Normal University, Nanjing 210023, China

* Corresponding author

E-mail addresses: wanghy419@csu.edu.cn (Haiyan Wang)

Experimental Section

1. Synthesis of Solid-State Electrolytes

Li_3InCl_6 (abbreviated as LIC) was prepared by ball-milling. LIC was synthesized by ball-milling a mixture of lithium chloride (LiCl, Sigma Aldrich, 99%) and indium chloride ($InCl_3$, Sigma Aldrich, 99.99%) at a 3:1 molar ratio under an argon (Ar) atmosphere at 500 rpm for 12 hours. To enhance the crystallinity of LIC, the ball-milled powder was sintered at 300 ℃ for 5 hours, producing LIC@300 ℃. Note that, unless otherwise specified, all SSEs tested in this study were ball-milled LIC without thermal treatment.

The argyrodite Li_6PS_5Cl (denoted as LPSC) was prepared by the ball-milling method. First, lithium sulfide (Li_2S, Sigma Aldrich, 99.98%), phosphorus pentasulfide (P_2S_5, Sigma Aldrich, 99%), and lithium chloride (LiCl, Sigma Aldrich, 99%) were mixed in a 5:1:2 molar ratio and ball-milled for 12 hours at 500 rpm in an Ar atmosphere. The resulting powder was then sintered at 550 ℃ under an Ar atmosphere for 5 hours to prepare LPSC.

2. Pre-treatment of lithium metal anodes

A CR2016-type Li|Li symmetric coin cell was assembled using an electrolyte consisting of 1 M $LiPF_6$ in DME:EC:EMC (1:1:1 by volume) with 5 vol% FEC additive. The cell was subjected to one galvanostatic charge–discharge cycle at a current density of 0.02 mA cm^{-2} and a capacity limit of 0.2 mAh cm^{-2}. After cycling, the cell was carefully disassembled. The metallic lithium anode was retrieved and thoroughly rinsed to remove any residual electrolyte, yielding the final pretreated lithium anode.

3. Material Characterization

The crystal structures of SSEs were confirmed by powder X-ray diffraction (XRD, SmartLab

3kW, Rigaku Corporation) using Cu-Kα radiation. The microscopic morphology of the materials was observed using field emission scanning electron microscopy (FE-SEM, TESCAN MIRA3), while the elemental distribution of the samples was determined using energy dispersive spectroscopy (EDS, Bruker Quantax 6|30 detector). X-ray photoelectron spectroscopy (XPS) measurements were performed on a Thermo Fisher Scientific NEXSA system.

4. Electrochemical Measurements

Conductivity measurements: Ionic conductivity was measured by cold-pressing 100 mg of SSE powder into pellets using a polyetheretherketone (PEEK) mold (inner diameter: 10 mm) under a pressure of 450 MPa. Stainless steel ion-blocking electrodes were employed. Electrochemical impedance spectroscopy (EIS) was performed using an electrochemical workstation (Multi Autolab/M204) over a frequency range of 1 MHz to 1 Hz to obtain Nyquist plots. The temperature-dependent ionic conductivity was measured between 20 and 60 ℃, and the activation energy was calculated using the Arrhenius equation. For the bilayer SSE, 40 mg of LPSC powder was first pre-compressed at 100 MPa. Subsequently, 60 mg of LIC powder was added, and the bilayer pellet was cold-pressed at 450 MPa for ionic conductivity testing.

Battery assembly and testing: All-solid-state lithium metal batteries were assembled in an argon-filled glove box (H_2O < 0.1 ppm, O_2 < 0.1 ppm). The composite cathode was prepared by uniformly mixing commercial lithium cobalt oxide (LCO) powder with halide SSE powder at a 7:3 mass ratio in an agate mortar. For cell assembly, 40 mg of sulfur-based SSE (LPSC) powder was added to a PEEK mold (10 mm inner diameter) and pressed at ~100 MPa to form the first electrolyte layer. Subsequently, 60 mg of LIC powder was added on the LPSC layer and cold-pressed at ~100 MPa to form a bilayer electrolyte structure. Approximately 10.5 mg of the composite cathode

powder was then uniformly distributed onto the LIC layer and pressed at ~450 MPa for 10 minutes to ensure interfacial adhesion. Finally, a lithium metal anode (either Li or FEC@Li, 10 mm in diameter) was placed on the LPSC side and pressed at ~60 MPa to ensure contact. The cells were cycled between 2.6 and 4.2 V (vs. Li/Li^+) at 30 °C using a NEWARE battery testing system to evaluate their rate capability and cycling performance.

5. Density Functional Theory Calculation

The highest occupied molecular orbital (HOMO) and lowest unoccupied molecular orbital (LUMO) energy levels of the solvent molecules were calculated using the DMol^3 module in Materials Studio 2021 (Accelrys Inc.).[s1] All structures underwent geometry optimization followed by orbital energy calculations within the DMol³ module. The exchange-correlation functional was described by the Becke three-parameter hybrid functional combined with the Lee-Yang-Parr correlation functional (B3LYP).[s2] Calculations employed an all-electron numerical basis set (Double Numerical plus polarization, DNP) with a basis file version 4.4. The Tkatchenko-Scheffler (TS) method was applied for van der Waals corrections.[s3] Convergence criteria were set to: 1.0×10^{-5} Ha for energy, 2.0×10^{-3} Ha $Å^{-1}$ for maximum force, and 5.0×10^{-3} Å for maximum displacement.

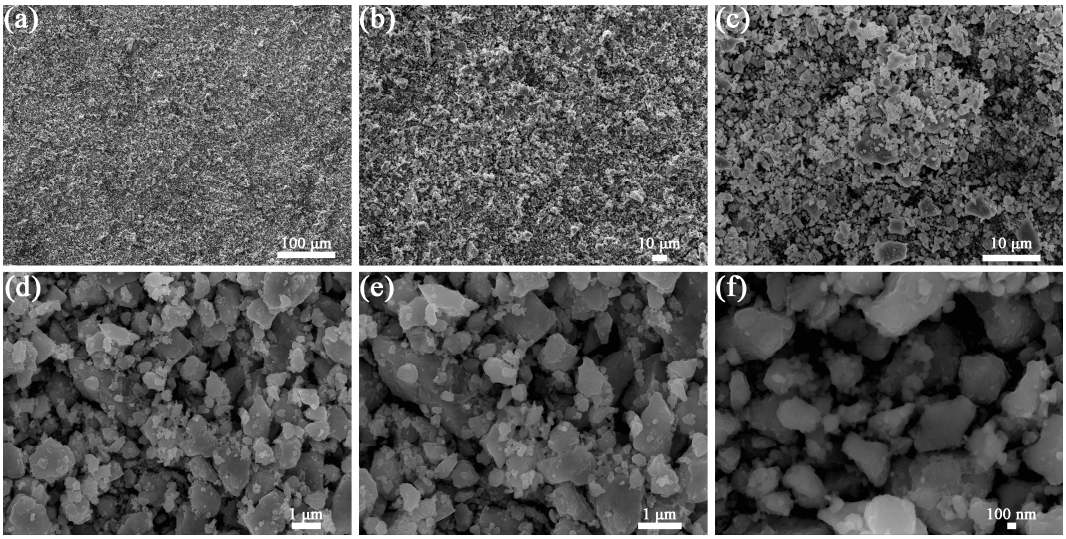

Fig. S1. SEM images of Li_3InCl_6 at different magnifications.

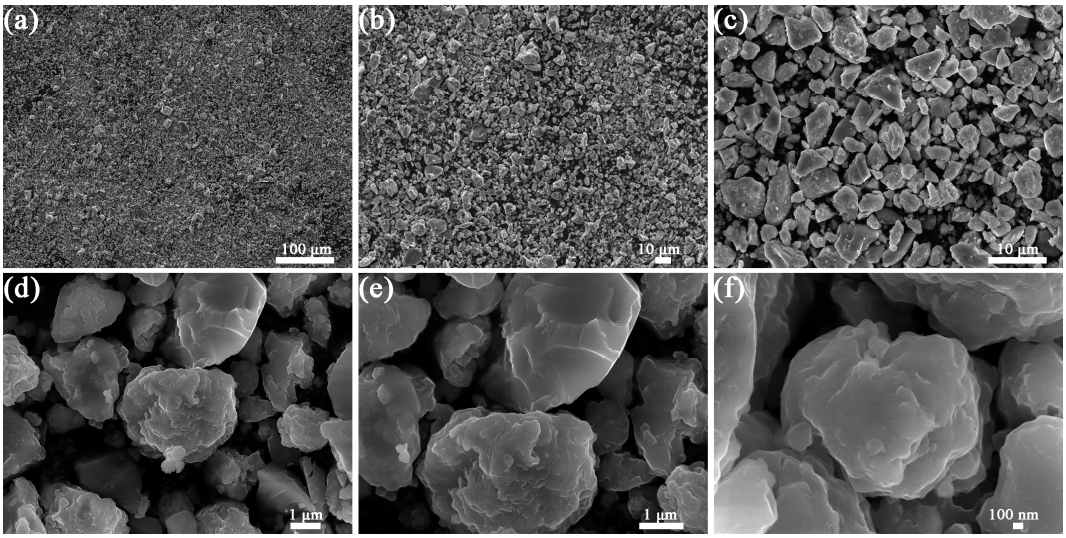

Fig. S2.SEM images of Li_6PS_5Cl at different magnifications.

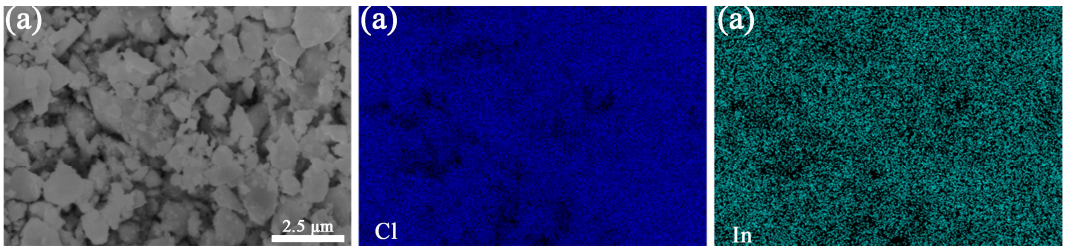

Fig. S3. EDS mapping images of Li_3InCl_6.

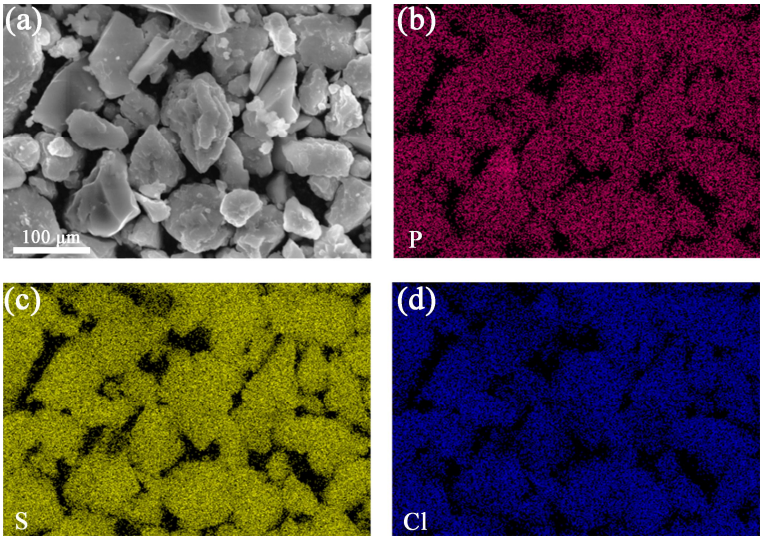

Fig. S4. EDS mapping images of Li_6PS_5Cl.

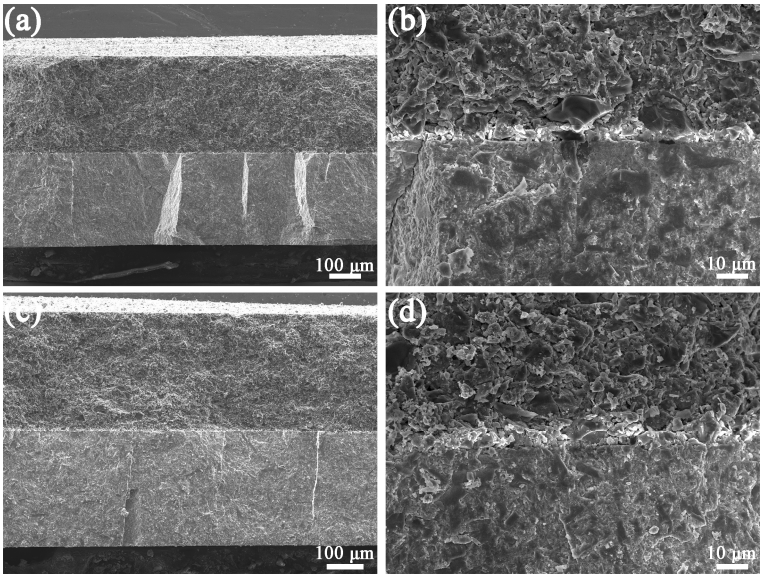

Fig. S5. SEM images of the cross-section of the bilayer SSE at different magnifications.

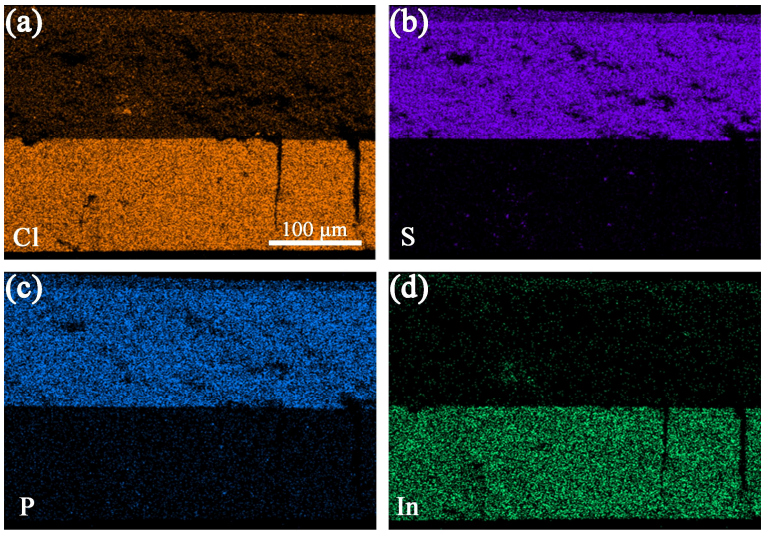

Fig. S6. EDS mapping images of the cross-section of the bilayer SSE.

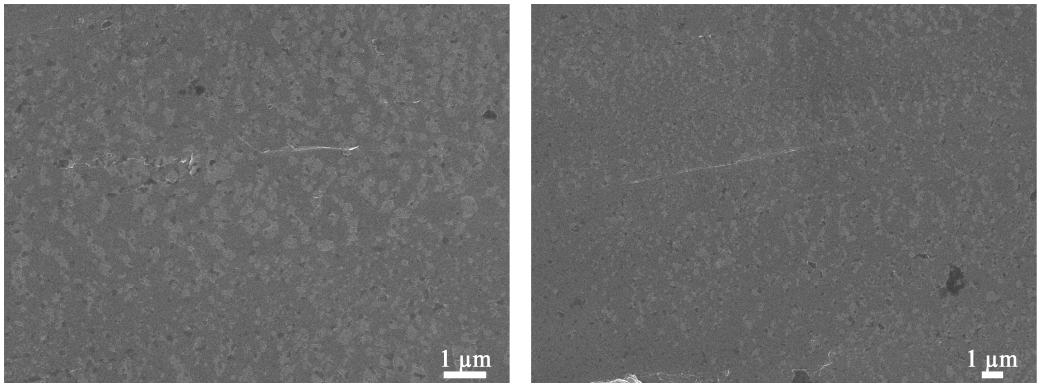

Fig. S7. SEM images of the surface of bare Li.

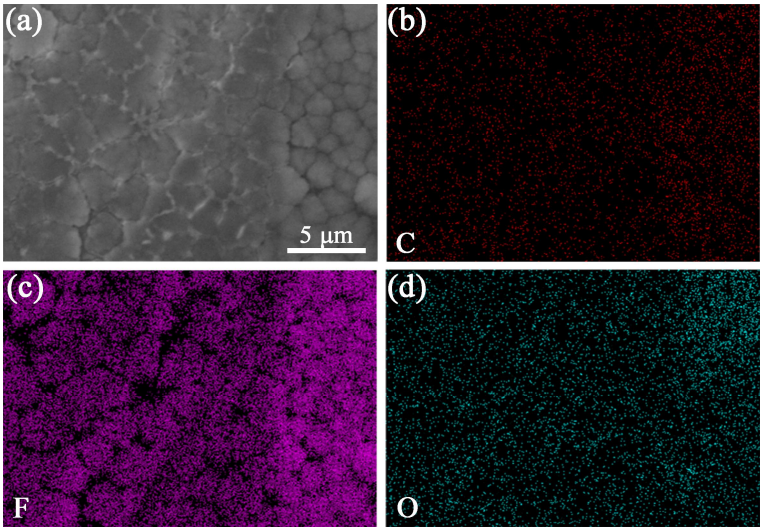

Fig. S8. EDS mapping images of the FEC@Li surface.

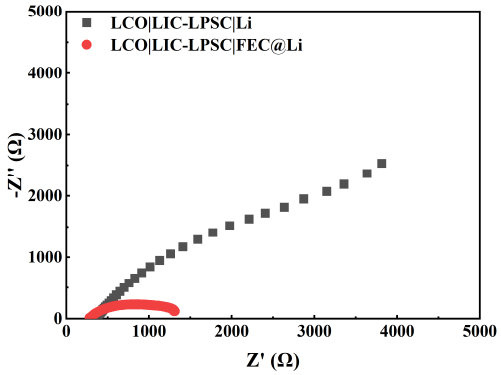

Fig. S9. EIS curves of LCO|LIC-LPSC|Li and LCO|LIC-LPSC|FEC@Li batteries.

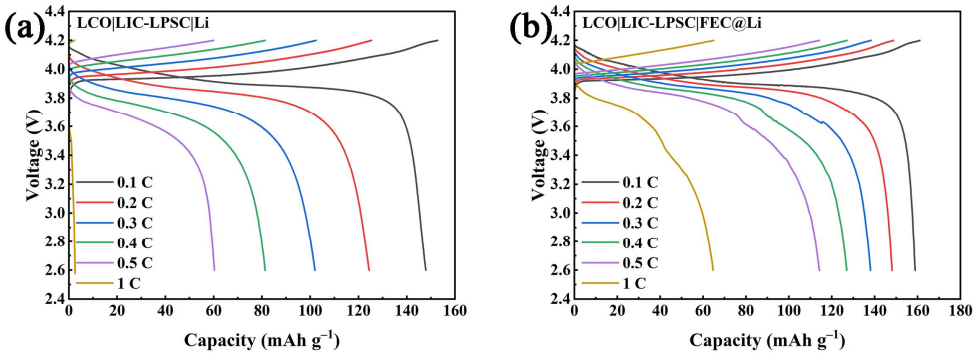

Fig. S10. Charge and discharge curves of LCO|LIC-LPSC|Li and LCO|LIC-LPSC|FEC@Li batteries at different rates.

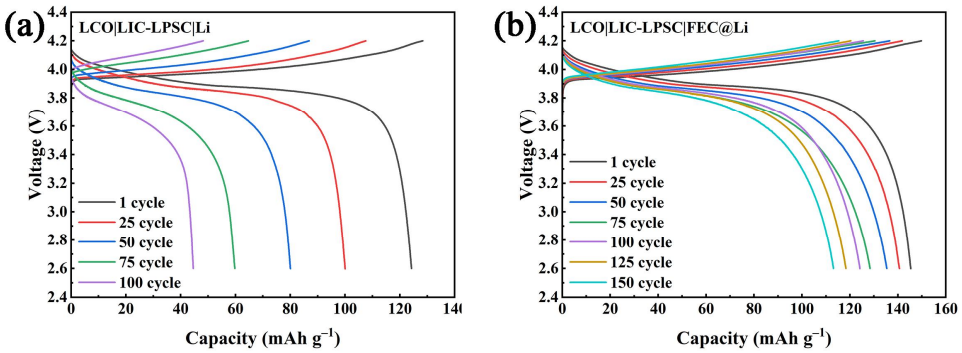

Fig. S11. Charge and discharge curves of LCO|LIC-LPSC|Li and LCO|LIC-LPSC|FEC@Li batteries at 0.2 C.

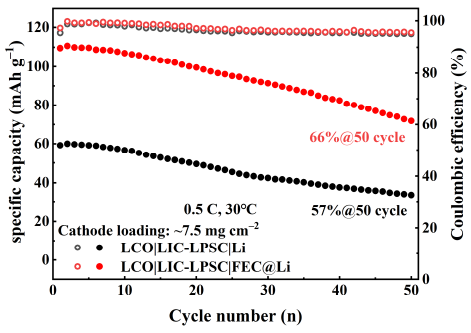

Fig. S12. Long cycle performance of LCO|LIC-LPSC|Li and LCO|LIC-LPSC|FEC@Li batteries.

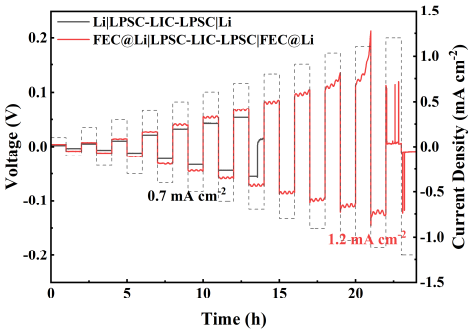

Fig. S13. The CCD test of symmetric cells with stepwise-increased current density.

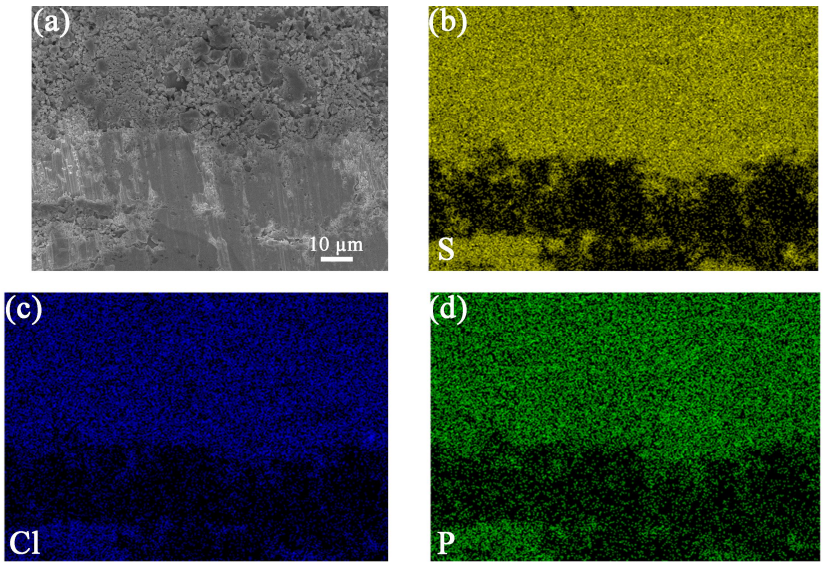

Fig. S14. (a) Cross-sectional SEM image and (b-d) corresponding EDS elemental maps images of the FEC@Li | LPSC | FEC@Li symmetric cell after cycling for 20 h at 0.3 mA cm^{-2}.

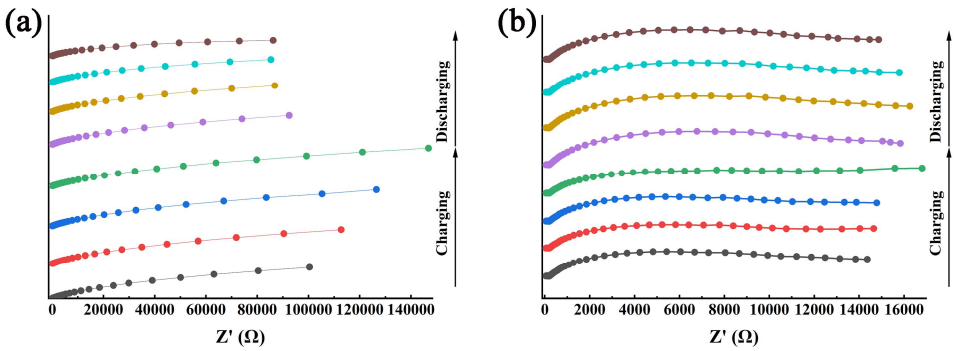

Figure S15. In situ EIS curves of Li|LPSC|Li and FEC@Li|LPSC|FEC@Li symmetric cells.

References

1. B. Delley, *The Journal of Chemical Physics*, 2000, **113**, 7756-7764.
2. A. D. Becke, *The Journal of Chemical Physics*, 1992, **96**, 2155-2160.
3. A. Tkatchenko and M. Scheffler, *Physical Review Letters*, 2009, **102**, 073005.